2013

Direct ignition and S-curve transition by *in situ* nano-second pulsed discharge in methane/oxygen/helium counterflow flame

Wenting Sun
Princeton University, wentings@princeton.edu

Sang Hee Won
Princeton University

Timothy Ombrello
Wright-Patterson AFB

Campbell Carter
Wright-Patterson AFB

Yiguang Ju
Princeton University

Available online at www.sciencedirect.com

SciVerse ScienceDirect

Proceedings of the Combustion Institute 34 (2013) 847–855

Proceedings of the Combustion Institute

www.elsevier.com/locate/proci

Direct ignition and *S*-curve transition by *in situ* nano-second pulsed discharge in methane/oxygen/helium counterflow flame

Wenting Sun [a,*], Sang Hee Won [a], Timothy Ombrello [b], Campbell Carter [b], Yiguang Ju [a]

[a] *Department of Mechanical and Aerospace Engineering, Princeton University, Princeton, NJ 08544, USA*
[b] *U.S. Air Force Research Laboratory, Propulsion Directorate, Wright-Patterson AFB, OH 45433, USA*

Available online 10 July 2012

Abstract

A well-defined plasma assisted combustion system with novel *in situ* discharge in a counterflow diffusion flame was developed to study the direct coupling kinetic effect of non-equilibrium plasma on flame ignition and extinction. A uniform discharge was generated between the burner nozzles by placing porous metal electrodes at the nozzle exits. The ignition and extinction characteristics of $CH_4/O_2/He$ diffusion flames were investigated by measuring excited OH^* and OH PLIF, at constant strain rates and O_2 mole fraction on the oxidizer side while changing the fuel mole fraction. It was found that ignition and extinction occurred with an abrupt change of OH^* emission intensity at lower O_2 mole fraction, indicating the existence of the conventional ignition-extinction *S*-curve. However, at a higher O_2 mole fraction, it was found that the *in situ* discharge could significantly modify the characteristics of ignition and extinction and create a new monotonic and fully stretched ignition *S*-curve. The transition from the conventional *S*-curves to a new stretched ignition curve indicated clearly that the active species generated by the plasma could change the chemical kinetic pathways of fuel oxidation at low temperature, thus resulting in the transition of flame stabilization mechanism from extinction-controlled to ignition-controlled regimes. The temperature and OH radical distributions were measured experimentally by the Rayleigh scattering technique and PLIF technique, respectively, and were compared with modeling. The results showed that the local maximum temperature in the reaction zone, where the ignition occurred, could be as low as 900 K. The chemical kinetic model for the plasma–flame interaction has been developed based on the assumption of constant electric field strength in the bulk plasma region. The reaction pathways analysis further revealed that atomic oxygen generated by the discharge was critical to controlling the radical production and promoting the chain branching effect in the reaction zone for low temperature ignition enhancement.

Keywords: Plasma assisted combustion; *In situ* discharge; Rayleigh scattering temperature measurement; Ignition; Extinction

* Corresponding author. Address: Department of Mechanical and Aerospace Engineering, Princeton University, D115, E-Quad, Olden St., Princeton, NJ 08544, USA.
E-mail address: wentings@princeton.edu (W. Sun).

1540-7489/$ - see front matter © 2012 The Combustion Institute. Published by Elsevier Inc. All rights reserved.
http://dx.doi.org/10.1016/j.proci.2012.06.104

1. Introduction

Over the few last years, plasma assisted combustion has drawn considerable attention for its potential to enhance combustion performance in internal combustion engines, gas turbines, and scramjet engines. Significant progress has been made in developing new techniques for plasma assisted combustion and in understanding the kinetic mechanisms of the plasma–combustion interaction [1–6]. However, due to the complexity of the interaction between plasma and flame kinetics, the fundamental kinetic enhancement mechanisms are not well understood.

Recently, much work has been conducted to understand the role of plasma generated species on ignition [1,2,7], flame speed enhancement [8,9] flame stabilization [4,5] and extinction [6,10]. For ignition studies, the reduction of ignition delay times by non-equilibrium nano-second pulsed discharges has been reported by applying the pulsed discharge prior to the arrival of the shockwave in a shock tube [2,11]. The results showed that the ignition delay times could be reduced by about an order of magnitude with the action of plasma due to the increase of atomic oxygen (O) concentration.

The efforts on quantitative understanding of the enhancement mechanism through the plasma/flame interaction has been made by several research groups [8,9,12,13]. Ombrello and co-workers experimentally isolated singlet oxygen $O_2(a^1\Delta_g)$ and ozone (O_3) from other plasma related species and have shown that both (at concentrations of several thousand ppm) can enhance flame speeds by a few percent [8,9]. Enhancement of flame stability by a non-equilibrium plasma in partially premixed systems have been observed for lifted flames [4,5]. Additionally, different explanations for plasma assisted combustion have been given, based on the production of H_2 and CO [5], as well as for the formation of active radicals such as OH and O [4].

Due to the complexity of directly coupling of the discharge with the flame, most of the experiments have been designed to isolate the direct coupling effect between the discharge and the flame, either temporally [2,3,11,14,15] or spatially [1,4–10,13,16], in order to elucidate the kinetic roles of species produced by the plasma. This isolation methodology has provided the unique advantage for the fundamental investigation on the kinetic role of plasma assisted combustion since the species generated by the plasma can be measured and transported to the combustion system, therefore isolating the effect of individual species. Recently, a well-defined counterflow system integrated with a nano-second pulsed discharge has been developed by applying the discharge on the oxidizer stream, and the effects of the discharge on the counterflow diffusion and partially premixed CH_4 flame extinction were studied [6,10]. Subsequent studies have revealed that the radicals/excited species generated by the plasma cannot be easily delivered to the main reaction zone, either because of the predominant recombination/quenching or due to the reactions with the doped fuel. Thus, the dominant effect of plasma on the reaction zone was not free from thermal enhancement effects, which would make the quantification of the kinetic enhancement mechanism difficult.

Motivated by this observation, the objective of this study is to investigate the direct coupling effect between plasma and a flame, where plasma kinetics pathways would modify the flame kinetic pathways. In order to focus on the kinetic performance of the plasma/flame interaction, a novel well-defined counterflow flame system with an *in situ* discharge has been developed. Direct kinetic coupling effects have been investigated both by experiments and numerical modeling. Further chemical kinetic aspects of the plasma/flame interaction are discussed through detailed flux analysis.

2. Experimental methods and numerical models

2.1. Counterflow flame and in situ nano-second pulsed discharge systems

A schematic of the experimental system is shown in Fig. 1. A counterflow burner was located in a low pressure chamber. Both the fuel and oxidizer nozzles of the counterflow burner were made of stainless steel with a 25.4 mm inner diameter. At the nozzle exits, stainless steel porous plugs (2 mm thickness) were placed to provide the uniform velocity profiles and to serve as the electrodes. The separation distance of the oxidizer and fuel burner nozzles (electrodes) was maintained at 16 mm. The oxidizer- and fuel-side electrodes were connected to the positive high voltage and the negative high voltage, respectively. The discharge could be generated between the two nozzles as shown in Fig. 1. The high voltage pulse was generated by a pulse generator with pulse duration of 12 ns (full width at half maximum, FWHM) and adjustable frequency. The voltage was measured by a high voltage probe (LeCroy, PPE20KV) and kept constant as 7.6 kV during the experiments. The current through the electrodes was measured with a Pearson Coil (Model 6585). The characteristics of voltage-current were found to be independent of the mixture compositions of the fuel and oxidizer sides. The pulse energy supplied to the discharge was estimated from the time integration of the voltage and current profiles and was found to be about 0.73 mJ/pulse. The pulse repetition frequency (f) was fixed at 24 kHz, corresponding to an input power of 17.5 W. In order to improve

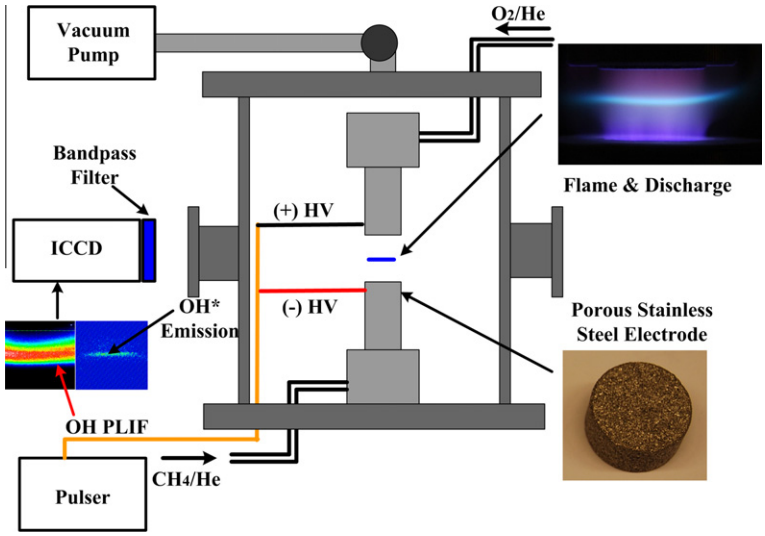

Fig. 1. Schematic of experimental setup.

the uniformity of the discharge, helium (He) was used as the dilution gas for both the fuel (CH_4) side and the oxidizer (O_2) side. The pressure was held constant at 9600 Pa for all of the experiments.

The temperature profiles were measured by the Rayleigh scattering technique [17] employing the second harmonic Nd:YAG laser beam at 532 nm. The laser sheet beam was produced by the combination of cylindrical lenses (focal length −50, 50 and 100 mm) to obtain two-dimensional images between the two nozzles of the counterflow burner. The Rayleigh scattering signals were collected by an ICCD camera (Princeton Instrument, PI-MAX) with a narrow band filter near 532 nm. To obtain a high signal to noise ratio, 1500 images were accumulated and averaged. The calibrations were conducted by comparing the signals with that from measurements with known composition, temperature and pressure. The cross sections of different species were accounted for in the Rayleigh scattering [18], and the mixture averaged cross sections were calculated using OPPDIF [19]. The maximum uncertainty of the Rayleigh scattering temperature measurements was found to be ±80 K, depending on the measurement location. The temperatures close to the burner surface (boundary temperatures) were measured by a thermocouple with three coating layers. The thermocouple was coated by magnesium oxide (MgO) on the surface and encapsulated by a metal sheath. So the electromagnetic effect from the pulsed discharge on the thermocouple could be removed. Finally, an aluminum oxide sheath (OD 3 mm) was used to cover the metal sheath to remove the effect from the ionized environment [20,21]. The thermocouple measurements were compared with Rayleigh scattering and other thermocouple measurements, with and without discharge, respectively. The uncertainty of the thermocouple measurements was found to be ±20 K.

2.2. Uniformity of the discharge and the excited OH emission from the reaction zone

The experiments were conducted by flowing a He/O_2 mixture from the top nozzle, and a He/CH_4 mixture from the bottom nozzle. The high voltage pulse applied on the electrodes could generate a uniform discharge between the two nozzles. The uniformity of the discharge could be confirmed by the single shot images from the ICCD camera (576-G/RB-E, Princeton Instruments) with a 50 ns gate, as shown in Fig. 2(a) and (b). It can be noted that no "hot spot" or filamentary discharge was observed with and without the flame, which allowed for a one-dimensional approach in the numerical simulations. Figure 2(c) and (d) also shows direct photos taken with a digital camera (Nikon, D40X) for the O_2 concentration (X_O) on the oxidizer side of 0.4. At the fixed strain rate, $a = 250$ 1/s, by gradually increasing the CH_4 concentration on the fuel side, X_F, the mixture is ignited at $X_F = 0.25$, and the resulting stable diffusion flame is shown in Fig. 2(c). Then by decreasing X_F, extinction is observed at $X_F = 0.14$, Fig. 2(d).

Considering that the ignition in the counterflow burner with heated air occurs generally at high temperatures (>1200 K) [22] and typical temperature variation of the current plasma configuration was below 1000 K [6,10], the above observation raises two fundamental questions. Firstly, what is the chemical kinetic mechanism for the ignition

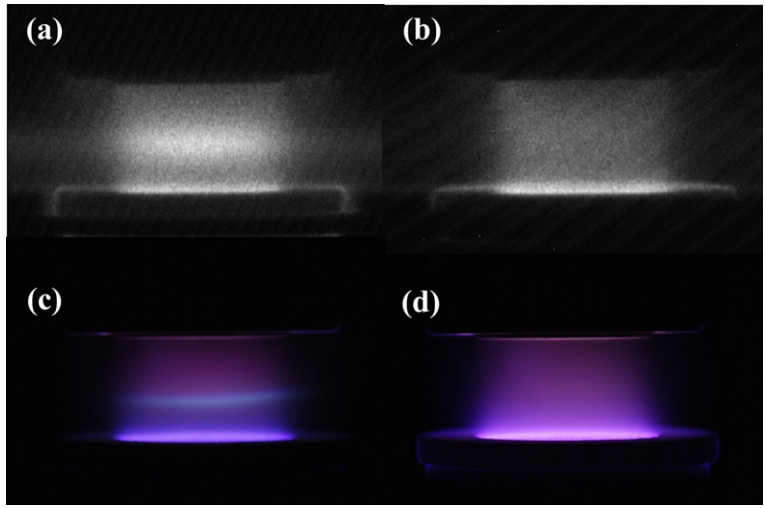

Fig. 2. (a) ICCD image at $X_O = 0.4$ and $X_F = 0.25$ diffusion flame and discharge, 50 ns gate; (b) ICCD image at $X_O = 0.4$ and $X_F = 0.14$ discharge, 50 ns gate; (c) direct photo of (a), 50 ms exposure time; (d) direct photo of (b), 50 ms exposure time, $P = 9600$ Pa, $f = 24$ kHz, $a = 250$ 1/s.

by the plasma? Secondly, how does the plasma and flame chemistry interact, thus changing the mechanisms of flame initiation and stabilization? In order to answer these two questions, the ignition by the plasma as a function of X_F was investigated by monitoring the intensity of excited OH (OH^*) emission as the flame or ignition marker [7,23] using the ICCD camera with a narrow bandpass filter, centered at 307 ± 2 nm (10 ± 2 nm FWHM). In order to suppress the emission of excited He at 315 nm, the ICCD camera gate (30 μs in all OH^* emission measurements) was delayed by 5 μs after the initial discharge pulse. A typical OH^* emission ICCD image is also embedded in Fig. 1. A flat reaction zone or flame between the nozzles can be identified clearly. The ignition and extinction limits were measured by varying X_F at several values of X_O in order to investigate the change of flame regimes with the activation of plasma. Finally, the chemical kinetic analysis was performed in order to address the plasma assisted ignition mechanism. In order to compare the difference between OH^* and OH density, OH planar laser induced fluorescence (OH PLIF) was used to measure the distribution of OH. The PLIF system consisted of an ND:YAG laser, a dye laser and an ICCD camera (Princeton Instrument, PI-MAX). The $Q_1(6)$ transition of OH was excited at the wavelength of 282.93 nm. More details about OH PLIF technique can be found in Ref. [24].

2.3. Kinetic modeling of plasma–flame interaction

The challenge of the modeling study of the plasma/flame interaction was whether the experimental observation could be properly simulated using a one-dimensional approximation. Although the diffusion flame in the counterflow configuration has been rigorously studied with a one-dimensional approximation [24–26], there still exists the open question on the validity of one-dimensional approximations for plasma properties. For example, the plasma properties, such as reduced electric field (defined as the local electric field strength, E, divided by the local number density, N) and species concentrations, may not be uniform in the radial direction of the counterflow burner. No detailed two- or three-dimensional computations have been done yet for plasma-flame systems due to the complex interaction of plasma/flame chemistry. Nevertheless, in our experiments, the OH^* profiles appeared to be uniform in the center region of the counterflow burner; this observation therefore rationalizes the one-dimensional approximation.

The kinetic mechanism was generated by the combination of a plasma kinetic model [3] and the combustion kinetic model, USC Mech II [27]. The details of the kinetic model can be found elsewhere [3,10], and only a brief summary is presented here. The reaction rate constants of electron impact related reactions are known to be a strong function of the reduced electrical field (E/N). These constants are generated independently by solving the steady state, two-term expansion Boltzmann equation for the electron energy distribution function (EEDF) of the plasma electrons, using the measured cross sections of electron impact on electronic excitation, dissociation, ionization, and dissociative attachment processes [10]. The current model does not solve the Poisson

equation for the electric field and therefore does not take into account for the charge separation and sheath formation near the electrodes. This modeling approach can be justified by the following reasons. In the present work, the voltage drops in the sheath regions close to the electrode surfaces are estimated by simulations at the same conditions but with homogeneous compositions [28,29]. The simulation shows that the electrical field ($E = 7500$ V/cm) in the bulk plasma region is nearly constant at different conditions as far as the applied voltage is constant, which was confirmed during the experiments. The typical electron density was approximately 5×10^{10} cm^{-3} in this study. Because the high voltage pulse is very short (12 ns) compared to the flow residence time, the flame cannot respond to the pulsed perturbation, and the pulsed excitation effect on the mixture is averaged over the fluid particles [30]. Finally, the kinetic mechanism that includes both plasma and combustion kinetics are generated and used by OPPDIF [19] to investigate their interactions.

3. Results and discussion

3.1. Observations of the S-curve transition

The ignition and extinction characteristics were studied by measuring the OH* emission intensity since ignition or extinction happens along with an abrupt change of the OH* emission. The integration of the OH* emission intensity across the reaction zone was used as a marker for comparisons of different cases/conditions. During the experiments, the strain rate (400 1/s, with flow residence time of approximately 2.5 ms) [1], X_O and the discharge frequency ($f = 24$ kHz) were held constant, while the CH_4 mole fraction on the fuel side, X_F, was varied. With varying the X_F, the thickness of the reaction zone was nearly a constant as marked by the OH* emission profile. For the first case, X_O was fixed at 0.34. The boundary temperatures of the oxidizer side and fuel side were 650 ± 20 K and 600 ± 20 K, respectively, and nearly constant through all the experiments with the fixed discharge frequency and experimental pressure. The relationship between OH* emission intensity as well as reaction zone peak temperature and X_F is shown in Fig. 3. The solid and open symbols in Fig. 3 represent the respective increasing and decreasing of X_F. By starting from $X_F = 0$ and increasing X_F until it equaled 0.265, the OH* emission was negligible compared to the background noise, and no reaction zone was observed. Further increase of X_F caused an abrupt increase of OH* emission intensity (from 0 to 8000 a.u.). This phenomenon was also identified by the appearance of a visible flame, indicating that ignition occurred. After ignition, further increase

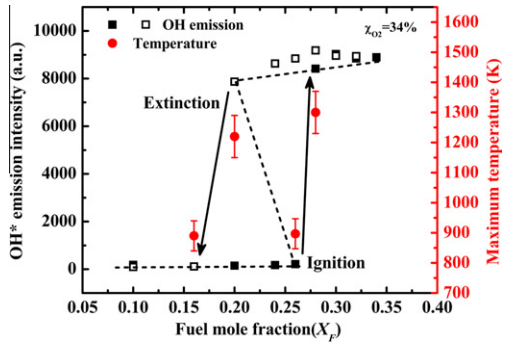

Fig. 3. Relationship between OH* emission intensity, local maximum temperature and fuel mole fraction, $X_O = 0.34$, P = 9600 Pa, $f = 24$ kHz, $a = 400$ 1/s (solid square symbols: increasing X_F, open square symbols: decreasing X_F).

or decrease of X_F only caused very limited increase or decrease of the OH* emission intensity, respectively. But if X_F is decreased to less than 0.20, an abrupt decrease of the OH* intensity was observed and the visible flame emission disappeared, indicating the extinction. This hysteresis of OH* emission intensity between ignition and extinction forms an *S*-curve of the flame [31], which is the fundamental phenomena of ignition and extinction. Similar curve can also be obtained by varying the discharge frequency with constant X_F and X_O If the discharge frequency was below 1 kHz, no ignition can be observed due to the quenching of radicals between two discharge pulses.

The local maximum temperature measurement (reaction zone temperature) showed that the value just before ignition was only 897 K, which was approximately 300 K higher than the boundary temperatures. The uncertainty of this measurement was about ± 50 K due to the repeatability of the experiments. With further increasing X_F, ignition occurred and the local maximum temperature increased to approximately 1310 K. At $X_F = 0$, the temperature distribution by Rayleigh scattering was nearly uniform without any local peak between the two burner nozzles, mostly due to the high diffusivity of helium at low pressure. The difference of temperature profiles with and without fuel flow indicated clearly (i) the existence of the coupling effects between the plasma and combustion chemistry for fuel oxidation and (ii) the consequent heat release at low temperatures to initiate ignition.

It has been shown [10] that plasma can initiate the CH_4 oxidation at low temperatures due to O generation from the discharge. More O generation will further enhance the fuel oxidization and ignition. Therefore, similar experimental observations were made by increasing X_O to 0.55 and 0.62 at the oxidizer side to increase O production. The results are shown in Figs. 4 and 5, respectively. Compared

to the results with $X_O = 0.34$ (Fig. 3), it was found that the hysteresis between ignition and extinction still existed for $X_O = 0.55$, but both the ignition and extinction points were pushed to lower fuel concentrations and become closer to each other: ignition was achieved at $X_F = 0.14$ and extinction did not occur until X_F was decreased to 0.1. Identical results were obtained by measuring the absolute OH number densities using OH PLIF in the reaction zone as provided in the Supplementary data, Fig. S1 with and without plasma. Without plasma, the OH concentration was significantly lower than that of with plasma and extinction happened at $X_F = 0.2$ without plasma. With a further increase in X_O to 0.62, the ignition and extinction points merged at $X_F = 0.09$, as shown in Fig. 5, and a monotonic ignition and extinction *S*-curve was formed. The temperature measurements also demonstrated a similar monotonic increase of the local maximum temperatures. The monotonic and fully stretched *S*-curve could be explained by the fact that the plasma generated reactive species caused a transition of flame stabilization mode from the extinction-controlled to the ignition-controlled modes. This means that the extinction limit did not exist by the plasma/combustion chemistry interaction, thus the chemistry of flame stabilization was fully dictated by the ignition limit. As a comparison, the pure thermal effect on the *S*-curve transition was investigated with numerical simulations by increasing the boundary temperatures of both the fuel and oxidizer sides. The details can be found in the Supplementary data, Fig. S2. It showed that the disappearance of ignition/extinction hysteresis could be observed at the extremely high boundary temperature of 1350 K. The electric power requirement to achieve 1350 K for both fuel and oxidizer is generally on the order of a kilowatt, which is significantly higher than the power consumption of 17.5 W by the plasma system.

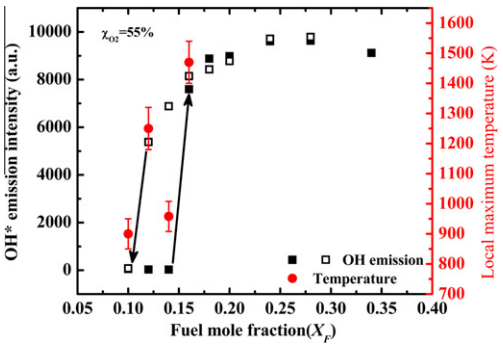

Fig. 4. Relationship between OH* emission intensity, local maximum temperature and fuel mole fraction, $X_O = 0.55$, $P = 9600$ Pa, $f = 24$ kHz, $a = 400$ 1/s (solid square symbols: increasing X_F, X_F, open square symbols: decreasing X_F).

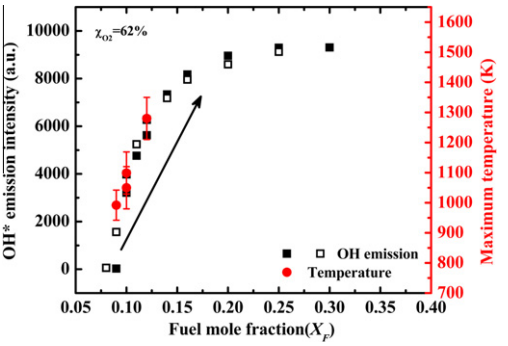

Fig. 5. Relationship between OH* emission intensity, local maximum temperature and fuel mole fraction $X_O = 0.62$, $P = 9600$ Pa, $f = 24$ kHz, $a = 400$ 1/s (solid square symbols: increasing X_F, open square symbols: decreasing X_F).

3.2. Numerical modeling results

The numerical simulations were conducted at the condition of $X_F = 0.16$ and $X_O = 0.34$ for the fuel and oxidizer sides, respectively, in order to analyze the plasma reactions prior to ignition and consequent formation of a flame. Without the plasma, no reaction (flame) could exist at this condition. With the presence of plasma, significant amounts of O, H and OH were generated as shown in Fig. 6(a); also shown are the measured and computed temperature profiles. Within the uncertainty of experiments (±50 K), the Rayleigh scattering measurement of the temperature agreed with the simulation. The deviations between the simulation and experiment close to the boundaries were larger since the Rayleigh scattering signals were inevitably overwhelmed by scattering from the burner surfaces. The temperature peaked near the stagnation plane, indicating the location of the main reaction zone. The O concentration peaked on the oxidizer side due to the direct electron dissociation of O_2, whereas the H peaks on the fuel side due to the electron dissociation of CH_4. The generation of O and H further stimulates the fuel oxidization to release chemical enthalpy, resulting in the temperature increase. The increased temperature in the reaction zone caused an increase of reduced electric field because of the constant electrical field (E) and decreased gas number density (N). Therefore, the increased E/N accelerated the direct electron impact reactions, as shown in Fig. 6(b), as the rate constants of direct electron impact reactions peaked also where the temperature peaked. The direct electron impact reactions further increased the heat release in the reaction zone. Therefore, it can be summarized that a positive feedback loop between the reaction zone and the discharge could be established by applying an *in situ* discharge to the system. Even though there was no flame, significant amounts (up to several thousand ppm

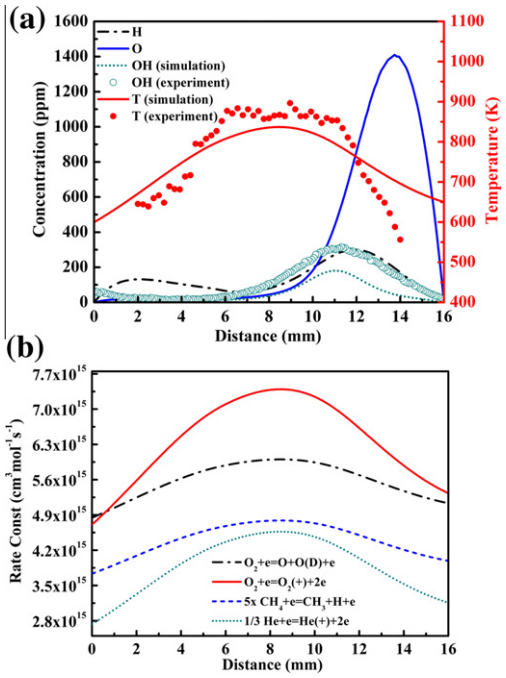

Fig. 6. (a) Radicals and temperature profiles without flame $X_F = 0.16$, $X_O = 0.34$, $P = 9600$ Pa, $f = 24$ kHz, $a = 400$ 1/s (fuel side at 0 mm, oxidizer side at 16 mm). (b) Rate constants of selected reactions for (a).

level) of H_2O, CO, CO_2 and H_2 were already formed in the reaction zone, which indicated the earlier heat extraction from the fuel by the plasma/combustion chemistry interaction.

In order to identify the important pathways of the radical generation and understand the kinetic processes in the plasma stimulated CH_4 oxidation mechanism, path flux analysis was performed; the details can be found in Supplementary data, Fig. S3. Approximately 7.3% of the CH_4 was ionized, but the quick charge transfer process between $CH_4(+)$ and O_2 canceled the effect of CH_4 ionization. CH_4 was predominantly dissociated to CH_3 by H abstraction through collision with OH, electrons, O and H. Approximately 24.5% of the CH_3 recombined to C_2H_6 due to the high concentration of CH_3 close to the fuel side. The major reaction path of CH_3 was the oxidization to CH_2O and finally to HCO, CO and CO_2. OH and H were predominantly generated through reactions between O and fuel/fuel-fragments. Therefore, it can be concluded that O was the initiation source of fuel oxidization and determined the population of the radical pool.

The dominant formation pathway of O was from direct electron impact of O_2, including reactions R1 to R3, and 57.9% of O was formed through these pathways:

$$e + O_2 = O + O(^1D) + e \quad (R1)$$

$$e + O_2 = 2O + e \quad (R2)$$

$$e + O_2 = O + O(+) + 2e \quad (R3)$$

Once $O(^1D)$ and O(+) were produced, they were quenched and recombined with electrons quickly to produce O, respectively. Another two important formation pathways of O were from collisions between O_2 and He ions (He(+)). Once O was formed, it reacted with CH_4 and its fragments to generate OH and H to further oxidize CH_4; only a small fraction of O recombined to form O_3 and O_2.

Since plasma was the source of radicals, the radical generation from the plasma could change the chain branching effects in the reaction zone. In order to demonstrate the change of branching effects in the reaction zone, the flux of radical generation was examined at constant $X_F = 0.16$ while varying X_O; the results are shown in Fig. 7. As the strongest radical generation reaction, R1 was chosen as the representative radical source from the plasma. Reaction R1 generated O which reacted with CH_4 to generate CH_3 and OH through reaction R4. Together with reaction R5, the generation of CH_3 promoted reaction R6 to generate H. The generation of H promoted the chain branching reaction R7 to generate OH and O and feed back to build up the radical pool:

$$CH_4 + O = CH_3 + OH \quad (R4)$$

$$CH_4 + OH = CH_3 + H_2O \quad (R5)$$

$$CH_4 + O = CH_2O + H \quad (R6)$$

$$H + O_2 = OH + O \quad (R7)$$

It is shown in Fig. 7 that by increasing X_O, the chain branching reaction R7 increased significantly, thus creating the larger radical pool population. Without plasma, the flame chemistry could not sustain the chain branching reaction below the crossover temperature for the flames, exhibiting

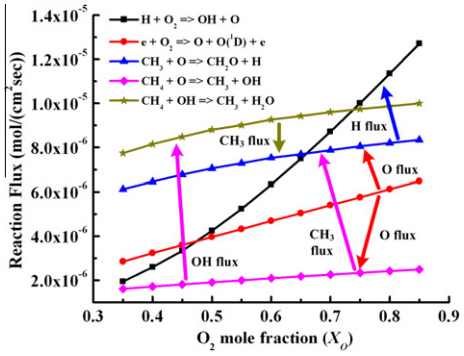

Fig. 7. Relationship of branching effects and O_2 concentration on the oxidizer side with fixed CH_4 mole fraction at $X_F = 0.16$.

hysteresis between ignition and extinction. However, the plasma enabled the chain branching reaction to be sustainable even at low temperatures by the positive loop between fuel oxidation and regeneration of the radical pool. Thus, the strong radical pool significantly decreased the global activation energy for fuel oxidation at low temperatures. Finally, the excessive production of radicals from the plasma diminished the hysteresis between ignition and extinction.

4. Conclusion

A novel well-defined plasma assisted combustion system with an *in situ* repetitive nano-second pulsed discharge integrated into counterflow flame has been developed by placing porous electrodes at the ends of the burner nozzles. Uniform discharge was generated between the two nozzles of the counterflow burner in CH_4/O_2/He diffusion flame. The new system provided an ideal platform to study the kinetic enhancement with the *in situ* discharge directly in the reaction zone so that the maximized kinetic enhancement effect by plasma could be observed at the increased reduced electrical field (E/N) in the reaction zone. The Rayleigh scattering temperature measurements have shown that the *in situ* discharge could dramatically reduce the CH_4 ignition temperatures as low as approximately 900 K. Unlike the conventional *S*-shaped ignition curve, a new stretched ignition to flame transition ignition curve was observed by measuring the excited OH^* emission and OH concentration. At $X_O = 0.34$ with fixed discharge frequency, a conventional *S*-curve with a clear hysteresis between the ignition and extinction limits was observed. However at higher oxygen concentration of $X_O = 0.62$, a direct transition of ignition and extinction diagram without the hysteresis was observed. The transition from the conventional to the fully stretched *S*-curves revealed that the radical pool population produced by the plasma significantly changed the chemical kinetic pathways of fuel oxidation, thus modifying the characteristics of ignition and extinction and the flame stabilization mechanisms. A kinetic model for plasma assisted methane/oxygen combustion has also been developed based on the assumption of constant electrical field strength. Numerical results demonstrate that O generation from the plasma was the dominant pathways to create the radical pool, such as H and OH. The path flux analysis revealed that the plasma and the subsequent interaction between plasma and combustion chemistries enabled the chain branching reaction to be sustainable even at low temperatures. The excessive production of radicals from the plasma decreased the global activation energy and removed the hysteresis of ignition and extinction. The results suggest that *in situ* repetitive non-equilibrium plasma assisted combustion can accelerate low temperature fuel oxidation at a high E/N ratio and can be potentially used to enhance ignition and combustion in high speed propulsion systems.

Acknowledgments

This work was supported by the MURI research grant from the Air Force Office of Scientific Research and the grant FA9550-07-1-0136. Wenting Sun thanks James Michael and Dr. Tanvir Farouk from the Department of Mechanical and Aerospace Engineering, Princeton University for the help of the Rayleigh scattering measurement and numerical modeling, respectively.

Appendix A. Supplementary data

Supplementary data associated with this article can be found, in the online version, at http://dx.doi.org/10.1016/j.proci.2012.06.104.

References

[1] T. Ombrello, Y. Ju, *IEEE Trans. Plasma Sci.* 36 (2008) 2924–2932.
[2] S.A. Bozhenkov, S.M. Starikovskaia, A.Y. Starikovskii, *Combust. Flame* 133 (2003) 133–146.
[3] M. Uddi, N. Jiang, E. Mintusov, I.V. Adamovich, W.R. Lempert, *Proc. Combust. Inst.* 32 (2009) 929–936.
[4] G. Pilla, D. Galley, D.A. Lacoste, F. Lacas, D. Veynante, C.O. Laux, *IEEE Trans. Plasma Sci.* 34 (6) (2006) 2471–2477.
[5] W. Kim, M.G. Mungal, M.A. Cappelli, *Combust. Flame* 157 (2) (2009) 374–383.
[6] W. Sun, M. Uddi, T. Ombrello, S.H. Won, C. Carter, Y. Ju, *Proc. Combust. Inst.* 33 (2011) 3211–3218.
[7] Z. Yin, I.V. Adamovich, in: *Forty-Ninth AIAA Aerospace Sciences Meeting including The New Horizons Forum and Aerospace Exposition*, Orlando, Florida, 2011.
[8] T. Ombrello, S.H. Won, Y. Ju, S. Williams, *Combust. Flame* 157 (2010) 1906–1915.
[9] T. Ombrello, S.H. Won, Y. Ju, S. Williams, *Combust. Flame* 157 (2010) 1916–1928.
[10] W. Sun, M. Uddi, S.H. Won, T. Ombrello, C. Carter, Y. Ju, *Combust. Flame* 159 (2012) 221–229.
[11] N.L. Aleksandrov, S.V. Kindysheva, I.N. Kosarev, S.M. Starikovskaia, A.Y. Starikovskii, *Proc. Combust. Inst.* 32 (2009) 205–212.
[12] A.M. Starik, V.E. Kozlov, N.S. Titova, *Combust. Flame* 157 (2) (2009) 313–327.
[13] X. Rao, K. Hemawan, I. Wichman, et al., *Proc. Combust. Inst.* 33 (2011) 3233–3240.
[14] A. Bao, Y. G Utkin, S. Keshav, G. Lou, I.V. Adamovich, *IEEE Trans. Plasma Sci.* 35 (6) (2007) 1628–1638.

[15] L. Wu, N.P. Cernansky, D.L. Miller, A.A. Fridman, A.Y. Starikovskiy, *Proc. Combust. Inst.* 33 (2011) 3219–3224.
[16] S.V. Pancheshnyi, D.A. Lacoste, A. Bourdon, C.O. Laux, *IEEE Trans. Plasma Sci.* 34 (6) (2006) 2478–2487.
[17] B. Bork, B. Böhm, C. Heeger, S.R. Chakravarthy, A. Dreizler, *Appl. Phys. B* 101 (2010) 487–491.
[18] W.C. Gardiner, J.Y. Hidaka, T. Tanzawa, *Combust. Flame* 40 (1981) 213–219.
[19] R.J. Kee, F.M. Rupley, J.A. Miller, et al., *Chemkin Collection, Release 3.7.1*, Reaction Design Inc., San Diego, CA, 2003.
[20] C.A.M. Mouwen, J.G.A. Holscher, *Physica* 73 (1974) 403–414.
[21] A.I. Maksimov, A.F. Sergienko, D.I. Slovetskii, *Sov. J. Plasma Phys.* 4 (1978) 194–197.
[22] T. Ombrello, Y. Ju, A. Fridman, *AIAA J.* 46 (10) (2008) 2424–2433.
[23] S.M. Starikovskaia, N.L. Aleksandrov, I.N. Kosarev, S.V. Kindysheva, A.Y. Starikovskiy, *High Energ. Chem+.* 43 (2009) 213–218.
[24] S.H. Won, W. Sun, Y. Ju, *Combust. Flame* 157 (2010) 411–420.
[25] O. Park, P. Veloo, N. Liu, F.N. Egolfopoulos, *Proc. Combust. Inst.* 33 (2011) 887–897.
[26] R. Grana, A. Frassoldati, T. Faravelli, et al., *Combust. Flame* 157 (2010) 2137–2154.
[27] H. Wang, X. You, A.V. Joshi, S.G. Davis, A. Laskin, F. Egolfopoulos, C.K. Law, available at http://ignis.usc.edu/USC_Mech_II.htm.
[28] T. Farouk, B. Farouk, A. Gutsol, A. Fridman, *Plasma Sources Sci. Trans.* 17 (2008) 035015.
[29] T. Farouk, B. Farouk, A. Gutsol, A. Fridman, *J. Phys. D Appl. Phys.* 41 (2008) 175202.
[30] A. Bao, *Ignition of Hydrocarbon Fuels by a Repetitively Pulsed Nanosecond Pulse Duration Plasma*, Ph.D. Dissertation, Mechanical Engineering Dept., Ohio State Univ., Columbus, OH, 2008.
[31] F.E. Fendell, *J. Fluid Mech.* 21 (1965) 281–303.